Received: 25 August 2020 | Accepted: 29 December 2020

DOI: 10.1111/bpa.12935

Brain Pathology

RESEARCH ARTICLE

# Mediators of cerebral hypoperfusion and blood-brain barrier leakiness in Alzheimer's disease, vascular dementia and mixed dementia

**Hannah Tayler** | **J. Scott Miners** | **Özge Güzel** | **Rob MacLachlan** | **Seth Love**

Dementia Research Group, Institute of Clinical Neurosciences, Bristol Medical School, University of Bristol, Bristol, UK

**Correspondence**
Seth Love, Translational Health Sciences, Bristol Medical School, University of Bristol, Learning & Research level 2, Southmead Hospital, Bristol BS10 5NB, UK.
Email: Seth.Love@Bristol.ac.uk

**Funding information**
This study was funded by Alzheimer's Research UK grants ARUK-PG2015-11 and ARUK-NAS2016B-1

## Abstract

In vascular dementia (VaD) and Alzheimer's disease (AD), cerebral hypoperfusion and blood-brain barrier (BBB) leakiness contribute to brain damage. In this study, we have measured biochemical markers and mediators of cerebral hypoperfusion and BBB in the frontal (BA6) and parietal (BA7) cortex and underlying white matter, to investigate the pathophysiology of vascular dysfunction in AD, VaD and mixed dementia. The ratio of myelin-associated glycoprotein to proteolipid protein-1 (MAG:PLP1), a post-mortem biochemical indicator of the adequacy of ante-mortem cerebral perfusion; the concentration of fibrinogen adjusted for haemoglobin level, a marker of blood-brain barrier (BBB) leakiness; the level of vascular endothelial growth factor-A (VEGF), a marker of tissue hypoxia; and endothelin-1 (EDN1), a potent vasoconstrictor, were measured by ELISA in the frontal and parietal cortex and underlying white matter in 94 AD, 20 VaD, 33 mixed dementia cases and 58 age-matched controls. All cases were assessed neuropathologically for small vessel disease (SVD), cerebral amyloid angiopathy (CAA) severity, Aβ and phospho-tau parenchymal load, and Braak tangle stage. Aβ40 and Aβ42 were measured by ELISA in guanidine-HCl tissue extracts. We found biochemical evidence of cerebral hypoperfusion in AD, VaD and mixed dementia to be associated with SVD, Aβ level, plaque load, EDN1 level and Braak tangle stage, and to be most widespread in mixed dementia. There was evidence of BBB leakiness in AD—limited to the cerebral cortex and related to EDN1 level. In conclusion, abnormalities of cerebral perfusion and BBB function in common types of dementia can largely be explained by a combination of arteriolosclerosis, and Aβ-, tau- and endothelin-related vascular dysfunction. The relative contributions of these processes vary considerably both between and within the diseases.

**KEYWORDS**
Alzheimer's disease, blood-brain barrier, cerebral hypoperfusion, mixed dementia, pathophysiology, vascular dementia

Hannah Tayler and J. Scott are contributed equally to this work.

This is an open access article under the terms of the Creative Commons Attribution-NonCommercial-NoDerivs License, which permits use and distribution in any medium, provided the original work is properly cited, the use is non-commercial and no modifications or adaptations are made.
© 2021 The Authors. *Brain Pathology* published by John Wiley & Sons Ltd on behalf of International Society of Neuropathology

# 1 | INTRODUCTION

Cerebral ischaemia is the defining pathogenic process that underlies vascular dementia (VaD), in which the ischaemia is usually secondary to small vessel disease (SVD). Cerebrovascular abnormalities are also common in patients with AD: over 90% have cerebral amyloid angiopathy (CAA) (1–3), and up to 60% have ischaemic white matter damage (4–7). Cerebral hypoperfusion (8,9) and blood-brain barrier (BBB) breakdown (10) can be detected prior to the onset of dementia and contribute to the cognitive decline in the early stages of AD (11). In familial AD (FAD), regional cerebral blood flow is reduced at least 10–15 years before the predicted onset of clinical symptoms, the spread of cerebral hypoperfusion mirroring the deposition and spread of Aβ (12). Ischaemic white matter damage can be demonstrated up to 20 years prior to the onset of clinical symptoms in FAD (13), and most of this damage seems to be independent of CAA (14).

A range of experimental studies has shown that brain ischaemia is likely to contribute to Aβ accumulation, through a combination of dysregulated processing and impaired clearance of Aβ [reviewed (15)]. In turn, Aβ peptides cause vasoconstriction, by inducing the contraction of pericytes (16) and probably vascular smooth muscle cells (17). Studies on rodent and human microvascular endothelial cell monolayers (18,19), human APP transgenic mouse models (20) and in human post-mortem brain tissue (21) also indicate that Aβ peptides directly impair BBB function, by reducing the expression of tight junction proteins including occludin and claudin. There is, therefore, a complex interrelationship between Aβ accumulation, reduced cerebral blood flow and BBB damage in AD in addition to VaD.

We previously explored the pathophysiology of cerebral ischaemia and BBB breakdown in VaD (22) and AD (23–25) by analysis of human post-mortem brain tissue. In those studies, ischaemic damage was quantified by comparing the levels of two myelin-proteins, myelin-associated protein (MAG) and proteolipid protein-1 (PLP-1), that are differentially susceptible to changes in tissue oxygenation (26). As both MAG and PLP1 have a similar, slow turnover in vivo (with half-lives of over 3 months) and are stable for 72 hr or more under post-mortem conditions (26), a reduction in the ratio of these proteins in post-mortem brain tissue indicates reduced perfusion of the tissue over a period of several months prior to death [reviewed in (27)]. We found the MAG:PLP1 ratio to be reduced in the white matter in VaD (22), and in the cerebral cortex in AD (23–25)—particularly in Braak tangle stage III and IV brains (24), i.e. at a relatively early stage of the disease. Reduced MAG:PLP1 in VaD and AD was generally associated with a concomitant increase in VEGF-A, an acute-response hypoxia-sensitive protein. MAG:PLP1 reduction and VEGF elevation correlated to some extent with the severity of cerebral amyloid angiopathy (CAA) and arteriosclerosis but were more strongly related to the level of endothelin-1 (EDN1) (24), a potent vasoconstrictor peptide, that we had shown previously to be increased in response to Aβ in AD (28). Within the precuneus, one of the earliest regions to show hypoperfusion in AD, the reduction of MAG:PLP1 was associated with loss of PDGFRβ, a pericyte marker, and an increase in fibrinogen (FG) within the brain tissue, indicating BBB damage (25). In that study, brain FG level correlated with the amounts of Aβ40 and Aβ42 in the tissue.

In the present study, we have further analysed vascular pathology and markers of vascular function in frontal and parietal cortex and white matter from neuropathologically defined cohorts of AD, VaD, mixed-dementia patients and age-matched controls, to identify disease-specific differences in the topography and pathophysiology of cerebral hypoperfusion and BBB breakdown. We have found cerebral hypoperfusion in AD, VaD and mixed dementia to be associated with small vessel disease, Aβ level, plaque load, EDN1 level and Braak tangle stage, and to be most widespread in mixed dementia. BBB leakiness was limited to the cerebral cortex in AD and was related to EDN1 level.

# 2 | METHODS

## 2.1 | Brain tissue

Intact frozen post-mortem human brain tissue from four regions: (i) frontal cortex (Brodmann area 6) and (ii) superficial underlying frontal white matter; (iii) precuneus (medial parietal cortex) (Brodmann area 7) and (iv) superficial underlying parietal white matter, was obtained from the South West Dementia Brain Bank for 58 controls with no significant cognitive impairment, 94 AD cases, 33 mixed dementia (AD and vascular) and 20 vascular dementia (VaD) cases. Neuropathological changes, according to National Institute on Ageing-Alzheimer's Association (NIA-AA) guidelines (29) were a sufficient explanation for Alzheimer's disease. VaD cases had a clinical history of dementia, only the occasional neuritic plaque and a Braak tangle stage of III or less, and histopathological evidence of multiple infarcts/ischaemic lesions, moderate to severe atheroma and/or arteriosclerosis, in the absence of histopathological evidence of other diseases likely to cause dementia. A neuropathological diagnosis of mixed dementia was made for dementia patients found at autopsy to have multiple infarcts/ischaemic lesions and moderate to severe atheroma, whilst also fulfilling NIA-AA criteria for AD. We excluded cases with Lewy body pathology. At the time of collection of some of the older brains used in this study, we did not routinely screen all brains for TDP43 pathology and so we have not included this in our analyses. Controls were age-matched, had no history of dementia,

**TABLE 1** Cohort summary

| | Control | Alzheimer's disease | Vascular dementia | Mixed dementia |
|---|---|---|---|---|
| N | 58 | 94 | 20 | 33 |
| Age (y) ± SD | 82.5 ± 9.1 | 77.7 ± 9.2 | 82.1 ± 7.8 | 87.3 ± 6.6 |
| Gender (M:F) | 33:25 | 51:43 | 10:10 | 9:24 |
| PM delay (h) ± SD | 41.5 ± 16.8 | 37.1 ± 19.3 | 44.2 ± 19.4 | 35.1 ± 16.7 |
| Braak tangle stage[a] | | | | |
| 0–II | 49 | 0 | 15 | 0 |
| III and IV | 8 | 12 | 5 | 10 |
| V and VI | 0 | 79 | 0 | 20 |

*Note:* Age and post-mortem (PM) delay are presented as the mean ± standard deviation (SD). The mean ages differed significantly between the groups (ANOVA, with Dunnett's test): the AD cases were significantly younger ($p < 0.001$) and the mixed dementia cases significantly older ($p < 0.05$) than the controls. There were more females in the mixed dementia group ($\chi^2$ (df 3) = 7.9657, $p = 0.047$). The mean PM delay was shorter in the AD and mixed dementia groups than in controls but the difference was not statistically significant (ANOVA).

[a]Braak tangle stage was not available for 1 control, 3 AD cases and 3 mixed dementia cases.

few or no neuritic plaques, and no other neuropathological abnormalities. Table 1 gives a summary of the cases included in each group.

## 2.2 | Assessment of Cerebral amyloid angiopathy (CAA) and small vessel disease (SVD) severity

CAA scores, based on the assessment of formalin-fixed paraffin-embedded sections of right frontal and parietal lobe immunolabelled with pan-Aβ 4G8 antibody (see below), were determined for the more recently donated cases in this study, or had been previously obtained (30). The CAA scores were based on the method of Olichney et al.,(31): 0 for vessels devoid of Aβ, 1 for limited deposits of vascular amyloid, 2 for the circumferential deposition of Aβ in several vessels, and 3 for severe and extensive CAA.

SVD (here used to refer specifically to arteriolosclerosis and excluding CAA) was scored in H&E-stained paraffin sections of right frontal and parietal lobe on a four-point semi-quantitative scale according to the level of arteriolar wall thickening and associated narrowing of vessel lumens: 0 for normal vessel wall thickness, 1 for slightly increased thickness, 2 for moderately increased thickness, and 3 for markedly increased thickness with concomitant reduction in many arteriolar lumina to less than 50% of the outer diameter of the vessel (26).

## 2.3 | Immunohistochemistry and analysis of parenchymal Aβ and tau load

The parenchymal Aβ and phospho-tau loads within the frontal (Brodmann area 6) and parietal cortex (Brodmann area 7) were determined in 7 μM sections immunolabelled with the pan-Aβ 4G8 antibody (32) and AT8 phospho-tau antibody (33), respectively. Both antibodies were optimised for use with an automated immunostainer (4G8 1:8000 and AT8 1:500 in PBS; Ventana BenchMark ULTRA, Roche Tissue Diagnostics). Aβ and phospho-tau loads were quantified by field-fraction analysis using computer-based image analysis software (Image-Pro Plus 7, Media Cybernetics). The Aβ and phospho-tau measurements are summarised in Table S1.

## 2.4 | ELISA measurements of insoluble Aβ40 and Aβ42

Insoluble (guanidine-extractable) fractions of the homogenates for Aβ measurement by ELISA were prepared as previously reported (23–25,34–37). Sandwich ELISA kits for the measurement of Aβ40 and Aβ42 (DAB140, DAB142; R&D Systems) were used according to the manufacturer's instructions. Brain homogenates were assayed in duplicate at 1:4000 dilution for cortical homogenates and 1:2500 for white matter homogenates. The levels of insoluble Aβ42 and Aβ40 in the frontal and parietal cortex and the underlying white matter are presented in Table S1.

## 2.5 | Biochemical assessment of vascular markers

### 2.5.1 | Brain tissue homogenisation

Brain tissue (200 mg) was homogenised in a Precellys homogeniser (2 × 15 s at 6000 rpm) with 5–10 silica beads (2.3 mm diameter) at 20% w/v in 1% SDS lysis buffer (1% w/v SDS, 0.1 M NaCl, 0.01 M Tris-HCl (pH 7.6), 1 μM PMSF and 1 μg/ml of aprotinin) for the measurement of MAG, PLP1, VEGF, FG, haemoglobin and EDN1 [as previously described (22–26)]. Homogenates were aliquoted and stored at −80°C prior to use.

### 2.6 | Myelin-associated glycoprotein (MAG) and proteolipid protein-1 (PLP1)

MAG level was measured in 1% SDS samples diluted 1 in 10 in PBS using an in-house developed direct ELISA as previously described (22–26). PLP1 level was measured in 1% SDS extracted brain tissue homogenates, diluted 1 in 10 in PBS, by use of a commercially available sandwich ELISA (SEA417Hu, USCN, Wuhan, China) as reported previously (22–26).

### 2.7 | Vascular endothelial growth factor-A (VEGF)

VEGF was measured by sandwich ELISA with the Human VEGF DuoSet (R&D Systems, DY293B), according to our previously published method (23-25).

### 2.8 | Fibrinogen (FG)

FG was measured in 1% SDS extracted brain tissue homogenates by a commercially available sandwich ELISA (FineTest EH3057 kit, Wuhan Fine Biotech Co., China) according to the manufacturer's instructions. Homogenate samples in SDS buffer were assayed in duplicate at 1:256 dilution for white matter and 1:128 for cortex. FG concentration was interpolated from a standard curve (1.563–100 ng/ml). As blood constitutes 4% and 5% of the volume of human brain tissue (38), FG measurements were adjusted for the haemoglobin content of the samples (see below), so that variation between samples largely reflected differences in extravascular FG content.

### 2.9 | Haemoglobin colorimetric assay

Haemoglobin was measured by a colorimetric assay kit (Cayman Chemicals), modified for assay in 384-well ELISA plates. Haemoglobin detector and standard (both supplied) were prepared according to kit instructions. Standards (0.016–0.4 g/dl) and blanks were loaded at 50 µL per well in triplicate. Samples (5 µl homogenate) and 45 µl detector reagent were loaded in triplicate. The plate was sealed and incubated for 15 min at RT and then the absorbance read at 590 nm. Sample haemoglobin concentration was determined by interpolation from the linear standard curve and adjusted for the dilution factor.

### 2.10 | Endothelin-1 (EDN1)

EDN1 was measured by QuantiGlo® ELISA for Human Endothelin-1 (R&D Systems, QET00B) as previously described (24). Homogenate samples in SDS buffer were assayed in duplicate at 1 mg/ml of total protein.

### 2.11 | Statistics

Unpaired two-tailed *t*-tests, or ANOVA with Dunnett's or Bonferroni post hoc analysis was used for comparisons between groups, and Pearson's or Spearman's test to assess linear or rank-order correlation, as appropriate, with the help of SPSS version 21 (SPSS, Chicago) and GraphPad Prism version 8 (GraphPad Software, La Jolla, CA). *p*-values <0.05 were considered statistically significant.

## 3 | RESULTS

### 3.1 | Biochemical assessment of cerebral hypoperfusion in VaD, AD and mixed dementia

In the frontal and parietal cortex, mean MAG:PLP1 was highest in controls and lowest in VaD, although the differences between VaD, AD, mixed dementia cases and controls were not statistically significant (Figure 1A,B). In frontal white matter, however, MAG:PLP1 was significantly lower in AD than controls ($p < 0.01$) (Figure 1C), and in parietal white matter, MAG:PLP1 was significantly lower in all dementia groups than in age-matched controls: AD ($p < 0.05$), VaD ($p < 0.01$) and mixed dementia ($p < 0.05$) (Figure 1D).

In all four regions examined, mean VEGF was lowest in controls and highest in mixed dementia. However, only in the frontal cortex and parietal white matter was the difference between controls and mixed dementia cases statistically significant ($p < 0.0001$ and $p < 0.001$, respectively) (Figure 2A–D). MAG:PLP1 and VEGF correlated inversely across all regions (Figure S1) as we have previously shown (22,24).

### 3.2 | BBB breakdown in the cerebral cortex in AD

Fibrinogen (FG), adjusted for haemoglobin content, was significantly elevated in the frontal cortex ($p < 0.05$), and was raised to a level approaching significance in the parietal cortex ($p = 0.09$) in AD compared to controls (Figure 3A,B). FG in the frontal and parietal cortex was unaltered in VaD and mixed dementia. FG was also unchanged in the white matter in any of the dementia groups (Figure 3C,D).

### 3.3 | Cortical hypoperfusion related to Aβ42, EDN1 and SVD

To gain insight into potential drivers of cerebral hypoperfusion in the dementia subgroups, we investigated whether biochemical markers of cerebral hypoperfusion (MAG:PLP1 and VEGF) were associated with insoluble Aβ level, parenchymal Aβ load, Braak tangle stage,

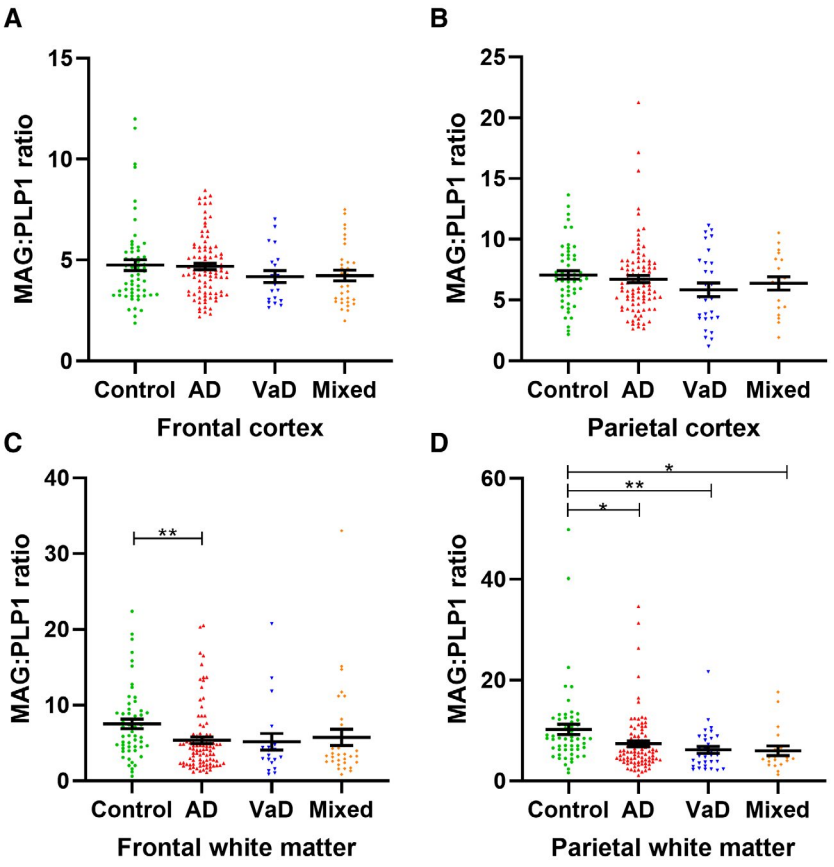


**FIGURE 1** Cerebral hypoperfusion in dementia. Scatterplots showing the ratio of myelin glycoprotein (MAG) to proteolipid protein-1 (PLP1) (MAG:PLP1) in the frontal and parietal cortex (A and B) and underlying white matter (C and D) in Alzheimer's disease (AD), vascular dementia (VaD), mixed dementia (mixed) and age-matched controls (Control). MAG:PLP1 was reduced in frontal white matter in AD and in the parietal white matter in AD, VaD and mixed dementia. Each dot represents the mean value in one brain. The horizontal bars indicate the mean ± standard error of the mean (SEM). *$p < 0.05$, **$p < 0.01$

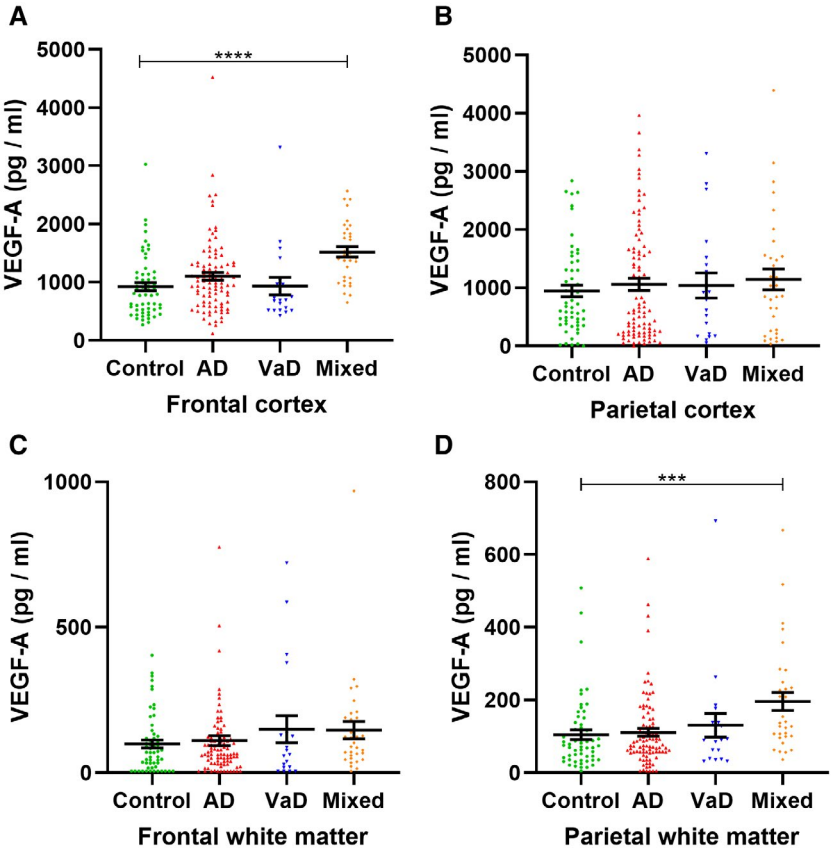


**FIGURE 2** Vascular-endothelial growth factor-A (VEGF-A) level is elevated in mixed (AD/VaD) dementia. Scatterplots showing the level of VEGF-A in the frontal and parietal cortex (A and B) and underlying white matter (C and D) in Alzheimer's disease (AD), vascular dementia (VaD), mixed dementia (mixed) and age-matched controls (Control). VEGF-A was elevated in mixed dementia in the frontal cortex and parietal white matter. Each dot represents the mean value in one brain. The horizontal bars indicate the mean ± standard error of the mean (SEM). $p$-values <0.05 were considered statistically significant. ***$p < 0.001$, ****$p < 0.0001$

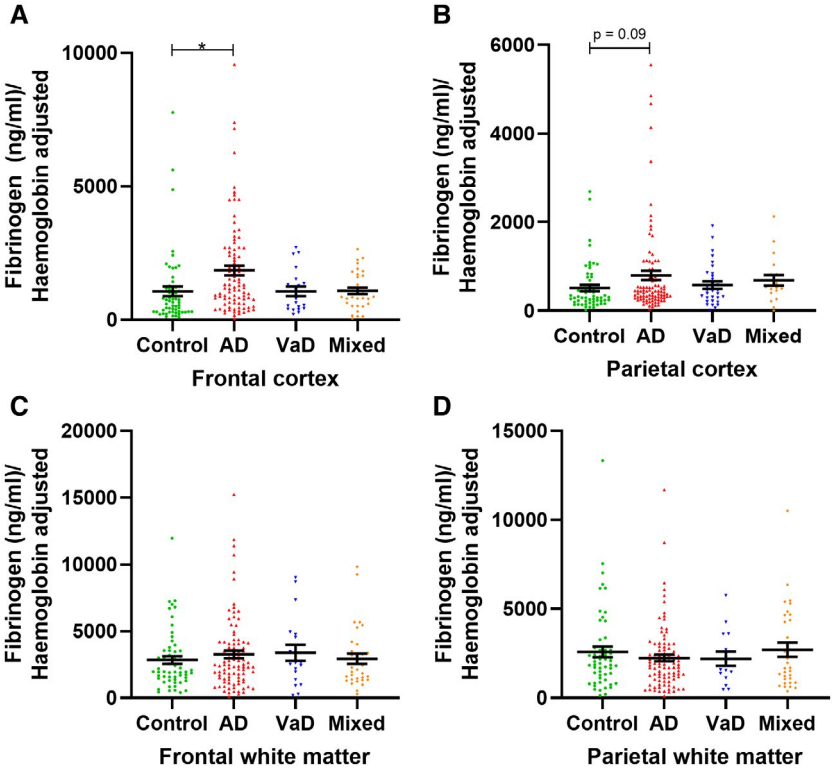


**FIGURE 3** Fibrinogen level is elevated in the cortex in Alzheimer's disease. Fibrinogen level, adjusted for haemoglobin content was measured in the frontal and parietal cortex (A and B) and underlying white matter (C and D) in Alzheimer's disease (AD), vascular dementia (VaD), mixed dementia (mixed) and age-matched controls (Control). Fibrinogen level was elevated in AD in the frontal cortex and to a level approaching significance in the parietal cortex. Each dot represents the mean value in one brain. The horizontal bars indicate the mean ± standard error of the mean (SEM). *p*-values <0.05 were considered statistically significant.
*$p < 0.05$

**TABLE 2** Cortical cerebral hypoperfusion is associated with insoluble Aβ42 and parenchymal Aβ load, and endothelin-1

| Cortical perfusion | MAG:PLP1 | | VEGF | |
|---|---|---|---|---|
| **Pearson coefficients** | **Frontal cortex** | **Parietal cortex** | **Frontal cortex** | **Parietal cortex** |
| Insoluble Aβ42 (pg/ml) | $r = -0.006$ | $r = -0.069$ | $r = 0.172^{*}$ | $r = -0.038$ |
| Insoluble Aβ40 (pg/ml) | $r = 0.031$ | $r = -0.061$ | $r = -0.071$ | $r = 0.031$ |
| Parenchymal Aβ load | $r = -0.022$ | $r = 0.007$ | $r = 0.249^{***}$ | $r = 0.011$ |
| Phospho-tau load | $r = -0.097$ | $r = -0.066$ | $r = 0.050$ | $r = 0.032$ |
| EDN1 (pg/ml) | $r = -0.13^{*}$ | $r = -0.037$ | $r = 0.23^{**}$ | $r = 0.293^{****}$ |

*Note:* Pearson's correlation coefficients are shown for the relationship of MAG:PLP1 or VEGF to levels of insoluble Aβ42 and Aβ40, parenchymal Aβ (4G8) and phospho-tau (AT8) load, and endothelin-1 (EDN1) level.
*$p < 0.05$; **$p < 0.01$; ***$p < 0.001$; ****$p < 0.0001$ denote statistically significant correlations.

phospho-tau load, EDN1 level, and severity of SVD and CAA.

In the frontal and parietal cortex, MAG:PLP1 did not correlate with insoluble Aβ42 or Aβ40, or parenchymal Aβ. However, VEGF level correlated positively with parenchymal Aβ load and with insoluble Aβ42 (but not Aβ40) in the frontal cortex. No correlations between VEGF and Aβ level or load were observed in the parietal cortex (Table 2 and Figure S2). Frontal and parietal MAG:PLP1 was not related to Braak tangle stage or parenchymal phospho-tau level. Frontal VEGF was increased in Braak stages III and IV vs 0-II, i.e. at an intermediate stage of progression of AD tangle pathology (Figure S3). MAG:PLP1 correlated inversely with EDN1 level in the frontal cortex but not the parietal cortex (Table 2 and Figure S3). VEGF level was strongly positively correlated with EDN1 in both the frontal and parietal cortex (Table 2). Frontal and parietal MAG:PLP1 and VEGF were not related to CAA severity. MAG:PLP1 tended to be reduced, and VEGF to be increased, in relation to the severity of SVD, although these trends did not reach significance (Figure S3). The relationships presented in Table 2 are shown as scatterplots in Figures S2 and S3.

### 3.4 | Subcortical white matter hypoperfusion related to EDN1 in the cortex and white matter, as well as Aβ parenchymal load and SVD severity

To gain insight into potential drivers of cerebral hypoperfusion of the white matter in the dementia subgroups,

we assessed whether white matter MAG:PLP1 and VEGF were associated with insoluble Aβ level (in both the white matter itself and in the overlying cortex, as the blood supply to the white matter is carried through perforating arterioles that traverse the cortex), parenchymal Aβ load, Braak tangle stage, phospho-tau load, EDN1 level in the white matter and overlying cortex, and severity of SVD and CAA.

MAG:PLP1 in the frontal white matter correlated inversely with insoluble Aβ42 level (but not Aβ40) in the cortex and with parenchymal Aβ load (Table 3 and Figure S4). White matter VEGF level did not vary significantly with Aβ42, Aβ40 or parenchymal Aβ in the cortex but did correlate positively with insoluble Aβ42 in the white matter in both the frontal and parietal lobes (Table 3 and Figure S4). In both the frontal and parietal white matter, MAG:PLP1 declined with increasing Braak tangle stage, being lower in BSV-VI than BS0-II (Figure S5), although white matter MAG:PLP1 did not vary significantly with phospho-tau level in the cortex. In contrast, white matter VEGF did not vary significantly with the Braak tangle stage but did correlate inversely with phospho-tau load in both regions of cortex (Table 3 and Figure S5).

MAG:PLP1 was inversely related to EDN1 level in the same samples of frontal and parietal white matter (Figure 4A,B). Frontal white matter MAG:PLP1 was also inversely related to EDN1 in the overlying cortex (Table 3). VEGF correlated positively with EDN1 in the same samples of frontal and parietal white matter (Figure 4C,D) but not with EDN1 in the overlying cortex. MAG:PLP1 in the frontal white matter was higher in cases with an SVD score of 0 than in those with a score of 1, 2, or 3 ($p < 0.05$ for all) but did not vary significantly between the other SVD subgroups (Table 3) or in relation to CAA severity in either region. VEGF in the white matter did not vary with the severity of CAA in the frontal or parietal lobe (Figure S5) or with SVD severity in the frontal lobe. However, VEGF was significantly higher in the parietal white matter in brains with severe SVD (i.e. a score of 3) than in those with less severe or absent SVD (Figure S5). Figures S4 and S5 show the relationships presented in Table 3 as individual scatterplots.

### 3.5 | Cortical BBB breakdown related to elevated EDN1

FG level, adjusted for haemoglobin content, correlated positively with EDN1 level in the frontal cortex (Figure 5A) and white matter (Figure 5B). FG level within the parietal cortex was not related to EDN1 level in the overlying cortex but correlated weakly with EDN1 in the underlying white matter (Figure 5C,D). FG level in the white matter did not correlate significantly with EDN1 in the cortex or white matter in either the frontal or parietal lobe.

## 4 | DISCUSSION

In this study, we have explored the distribution, and a range of possible contributors to, cerebral hypoperfusion and BBB breakdown in the parietal and frontal cortex and white matter in VaD, AD and mixed dementia. We found biochemical evidence of hypoperfusion in all three dementia subgroups but with differences in distribution and associated pathologies. In AD, evidence of hypoperfusion took the form of a reduced MAG:PLP1 ratio in the superficial subcortical white matter in both lobes. In VaD the reduction in MAG:PLP1 reached significance in the parietal white matter only. MAG:PLP1 was also reduced in the parietal white matter in mixed dementia but in this group there were also striking increases in VEGF in the frontal cortex as well as the parietal white matter. Across all cases, biochemical markers of cortical hypoperfusion and ischaemia, correlated with EDN1 level, parenchymal Aβ load and insoluble Aβ42 level. Subcortical

**TABLE 3** Subcortical hypoperfusion is associated with insoluble Aβ42 level and parenchymal Aβ load, and endothelin-1

| | MAG:PLP1 | | VEGF | |
|---|---|---|---|---|
| **Sub-cortical perfusion** | **Frontal white matter** | **Parietal white matter** | **Frontal white matter** | **Parietal white matter** |
| Insoluble Aβ42 (pg/ml) | $r = -0.187^{*}$ | $r = -0.096$ | $r = 0.019$ | $r = 0.055$ |
| Insoluble Aβ40 (pg/ml) | $r = -0.056$ | $r = -0.006$ | $r = -0.030$ | $r = -0.01$ |
| Parenchymal Aβ load | $r = -0.180^{*}$ | $r = -0.155^{*}$ | $r = 0.118$ | $r = -0.202^{*}$ |
| WM—Insoluble Aβ42 | $r = 0.092$ | $r = -0.067$ | $r = 0.165^{*}$ | $r = 0.140$ |
| Phospho-tau load | $r = -0.115$ | $r = 0.000$ | $r = -0.173^{**}$ | $r = -0.219^{***}$ |
| EDN1 (pg/ml) | $r = -0.189^{**}$ | $r = -0.043$ | $r = -0.051$ | $r = -0.078$ |
| WM—EDN1 (pg/ml) | $r = -0.233^{***}$ | $r = -0.190^{**}$ | $r = 0.173^{*}$ | $r = 0.29^{**}$ |

*Note:* Pearson's correlation coefficients are shown for the relationship of MAG:PLP1 or VEGF to levels of insoluble Aβ42 and Aβ40 in the white matter (WM) or cortex, parenchymal Aβ (4G8) and phospho-tau (AT8) load in the cortex, and white matter (WM) or cortical endothelin-1 (EDN1).

$^{*}p < 0.05$; $^{**}p < 0.01$; $^{***}p < 0.001$ denote statistically significant findings.

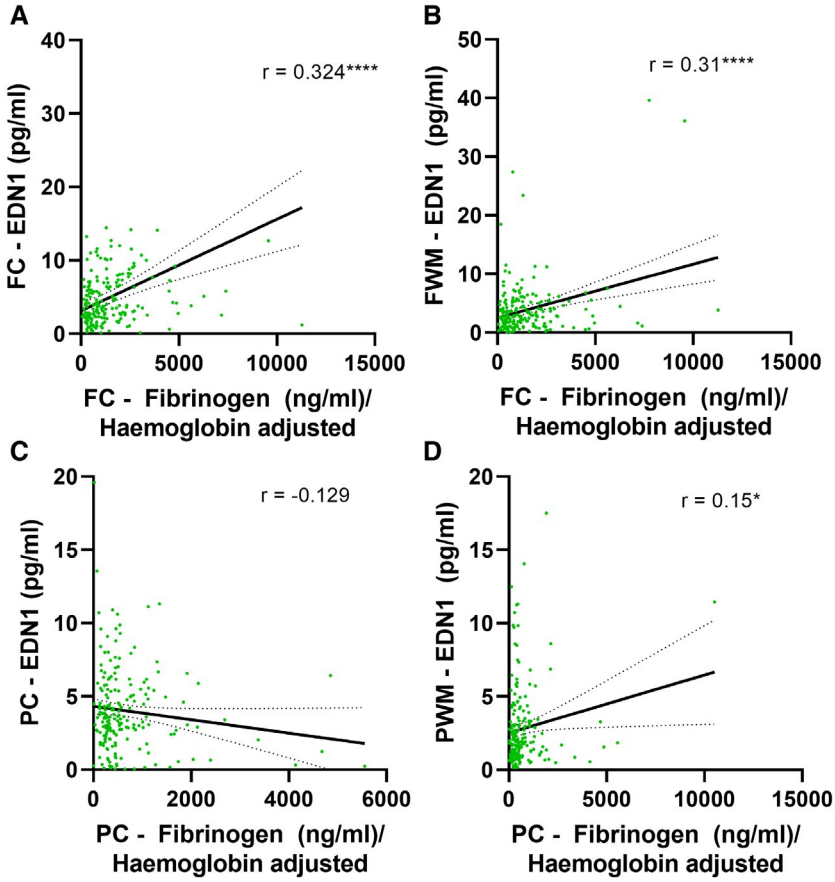


**FIGURE 5** Increased cortical fibrinogen, a marker of BBB damage, is associated with elevated cortical and subcortical endothelin-1 in Alzheimer's disease. (A–D) Scatterplots showing the relationship between fibrinogen level (adjusted for haemoglobin content) and cortical and subcortical endothelin-1 (EDN1) levels. The solid line indicates best-fit linear regression and the interrupted lines the 95% confidence intervals. Each point represents a separate brain. *$p < 0.05$, ****$p < 0.0001$

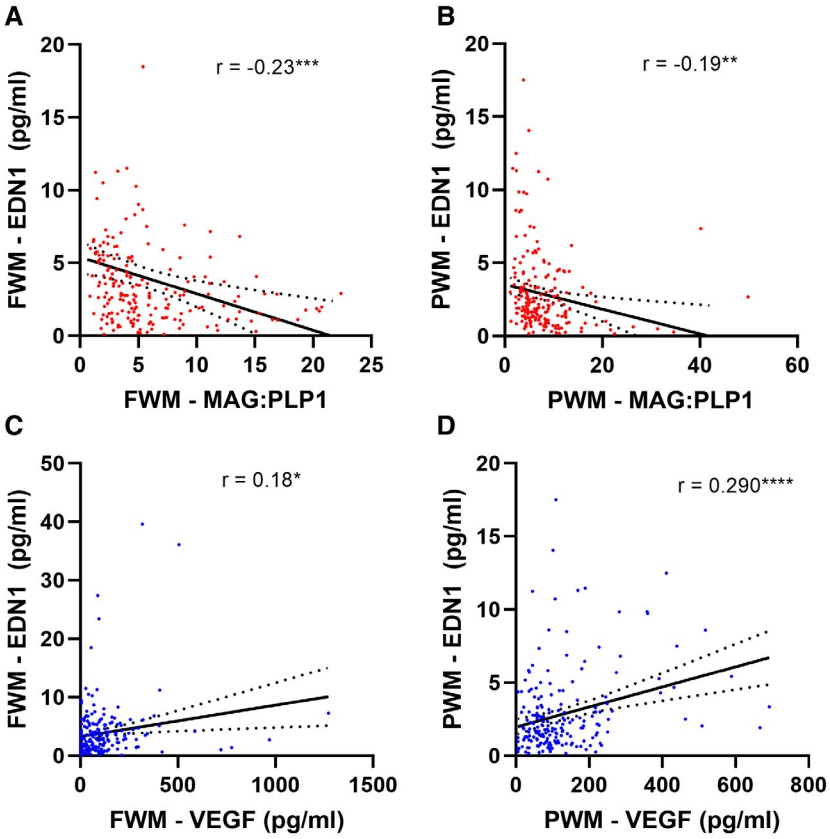


**FIGURE 4** Cerebral hypoperfusion of the white matter in Alzheimer's disease is related to endothelin-1 (EDN1). (A–D) Scatterplots showing the relationships between MAG:PLP1 (negative correlation) and VEGF (positive correlation) and endothelin-1 (EDN1) in the frontal and parietal white matter. The solid line indicates best-fit linear regression and the interrupted lines the 95% confidence intervals. Each point represents a separate brain. *$p < 0.05$, **$p < 0.01$, ***$p < 0.001$, ****$p < 0.0001$

hypoperfusion was related to SVD severity but was also associated with the levels of EDN1 and insoluble Aβ42 and with parenchymal Aβ load in the overlying cortex. FG was significantly elevated only in AD and only in the cortical regions and was related to the EDN1 level. These data suggest that there are multiple contributors to cerebral hypoperfusion in these common forms of dementia, but that BBB breakdown is more specifically a feature of AD, perhaps related to the overproduction of EDN1 within the cerebral cortex.

We previously reported biochemical evidence of cerebral hypoperfusion in post-mortem brain tissue in VaD and AD, indicated by a reduction in MAG:PLP1 and an increase in VEGF (reviewed (15,27)). These biochemical changes are pronounced in deep cerebral white matter from people with severe SVD (26) but can also be demonstrated in cortical regions and subcortical white matter in AD and VaD (22–24). In the medial parietal cortex, one of the first regions to demonstrate reduced blood flow in AD, MAG:PLP1 was much more reduced in Braak tangle stages III and IV than in later-stage disease, and was strongly related to EDN1 and Aβ42 level but only modestly to SVD and CAA severity (24). Cortical EDN1 and Aβ42 levels were also associated with hypoperfusion of the underlying frontal white matter perhaps as a result of EDN1-mediated constriction of perforating arterioles. Our present study largely confirms and extends those findings in a larger and more diverse cohort, emphasising the relationship between AD-related abnormalities (Aβ accumulation, Braak tangle stage and overproduction of EDN1) and both cortical and subcortical hypoperfusion, as well as the more modest but significant contribution of SVD to cerebral hypoperfusion in dementia.

One limitation of the present study is the modest size of the dementia subgroups, particularly the VaD subgroup. This is a reflection of the relative infrequency of neuropathologically confirmed VaD as a sole explanation for dementia, as noted in other autopsy studies (39,40). A further limitation is that we did not analyse TDP-43 pathology as a variable that might also be associated with cerebral hypoperfusion. There is evidence from recent studies that TDP-43 pathology may be associated with SVD (41,42) and it might, therefore, have been expected that MAG:PLP1 would be reduced and VEGF increased in brains showing TDP-43 pathology—this is something we will address in future studies. At present, it remains unclear what could be driving the reported association between TDP-43 pathology and SVD. In future studies we plan to investigate whether TDP-43 pathology, which tends to be most severe in the amygdala, hippocampus and medial temporal cortex, is associated with SVD, CAA and biochemical indicators of cerebral hypoperfusion and vascular insufficiency, including BBB leakiness and pericytes loss, and to examine the topographic relationships between these vascular and neuronal pathologies. Last, post-mortem preservation of proteins may influence the interpretation of the biochemical data, although in previous studies we have shown that most of the key vascular markers that we measured, including MAG, PLP1, VEGF and EDN1, are stable up to 72 hr at 4°C or even room temperature under conditions simulating post-mortem storage of human brain tissue (26,43).

In the present cohort, BBB leakiness, as indicated by increased FG, was limited to the frontal and parietal cortex and was specific to AD. We previously demonstrated that FG level is elevated in the precuneus in AD and that the elevation is associated with markers of cerebral hypoperfusion and the level of Aβ (25). FG level was also elevated in the parietal cortex and underlying white matter in AD (25). Here we found that cortical FG level was elevated in AD, but not significantly in the underlying white matter. Cortical FG correlated with EDN1 level in the frontal cortex. There is evidence from other studies that EDN1 increases BBB permeability. The binding of EDN1 to the endothelin-1 type A receptor (EDNRA) was shown to increase leakiness of the BBB in rats and dogs (44,45), and cognitive deficit and BBB leakiness were reported in transgenic mice overexpressing EDN1 (46). EDN1 also regulates monocyte diapedesis across the human endothelium (47). Leung et al. showed that EDN1 exacerbated BBB breakdown and oxidative damage after transient middle artery occlusion and that the damage was limited by the administration of EDNRA receptor antagonists (48). Upregulation of EDN1 production by oligomeric Aβ was also shown to cause pericyte-mediated capillary vasoconstriction (16) and to alter aquaporin-4 distribution in astrocyte end-feet (49). Together, these studies underline the likely contribution of Aβ-induced overproduction of EDN1 to BBB breakdown and vascular instability in AD. In contrast to AD, we did not find elevated FG levels in VaD in either the frontal or parietal cortex or underlying white matter. This was unexpected, in view of previous studies, indicating that vascular risk factors are associated with BBB leakiness in SVD and VaD in animal models and humans (50–52). Contributing factors may include the smaller size of the VaD cohort and the relatively advanced age of all of the cohorts, including the controls, many of which may have had some BBB leakiness independent of AD or VaD.

In conclusion, in the present study, we have identified disease-specific differences and commonalities in the topography and pathophysiology between biochemical markers of cerebral hypoperfusion and BBB breakdown across neuropathologically defined dementia sub-types. Differences in the severity and extent of vascular dysfunction in the cases studied largely reflect varied contributions from arteriolosclerosis, and Aβ-, tau and endothelin-related vascular dysfunction.

## ACKNOWLEDGEMENTS

We thank the South West Dementia Brain Bank (SWDBB) for providing brain tissue for this study. The SWDBB is part of the Brains for Dementia Research programme, jointly funded by Alzheimer's Research UK

and Alzheimer's Society and is supported by BRACE (Bristol Research into Alzheimer's and Care of the Elderly) and the Medical Research Council.

## CONFLICT OF INTEREST

The author(s) declare no potential conflicts of interest with respect to the research, authorship, and/or publication of this article.

## AUTHOR CONTRIBUTIONS

The study was devised by SL and JSM. HT, JSM, ÖG, RM and SL performed the analyses and collected the data. HT and JSM wrote the manuscript. SL undertook critical revision of the manuscript. All of the authors reviewed and approved the final manuscript.

## DATA AVAILABILITY STATEMENT

All data within the article are linked to the MRC UK-BBN by a unique numeric MRC UK-BBN identifier (Table S2).

## ORCID

*J. Scott Miners* https://orcid.org/0000-0001-8594-1640

## REFERENCES

1. Ellis RJ, Olichney JM, Thal LJ, Mirra SS, Morris JC, Beekly D, et al. Cerebral amyloid angiopathy in the brains of patients with Alzheimer's disease: the CERAD experience, part XV. Neurology. 1996;46(6):1592–6.
2. Esiri MM, Wilcock GK. Cerebral amyloid angiopathy in dementia and old age. J Neurol Neurosurg Psychiatry. 1986;49(11):1221–6.
3. Love S, Nicoll JA, Hughes A, Wilcock GK. APOE and cerebral amyloid angiopathy in the elderly. NeuroReport. 2003;14(11):1535–6.
4. Brun A, Englund E. Brain changes in dementia of Alzheimer's type relevant to new imaging diagnostic methods. Prog Neuropsychopharmacol Biol Psychiatry. 1986;10(3–5):297–308.
5. Brun A, Gustafson L, Englund E. Subcortical pathology of Alzheimer's disease. Adv Neurol. 1990;51:73–7.
6. Englund E. Neuropathology of white matter changes in Alzheimer's disease and vascular dementia. Dement Geriatr Cogn Disord. 1998;9(Suppl 1):6–12.
7. Kalaria RN. The role of cerebral ischemia in Alzheimer's disease. Neurobiol Aging. 2000;21(2):321–30.
8. Ruitenberg A, den Heijer T, Bakker SL, van Swieten JC, Koudstaal PJ, Hofman A, et al. Cerebral hypoperfusion and clinical onset of dementia: the Rotterdam Study. Ann Neurol. 2005;57(6):789–94.
9. Roher AE, Debbins JP, Malek-Ahmadi M, Chen K, Pipe JG, Maze S, et al. Cerebral blood flow in Alzheimer's disease. Vasc Health Risk Manag. 2012;8:599–611.
10. Montagne A, Barnes SR, Sweeney MD, Halliday MR, Sagare AP, Zhao Z, et al. Blood-brain barrier breakdown in the aging human hippocampus. Neuron. 2015;85(2):296–302.
11. Nation DA, Sweeney MD, Montagne A, Sagare AP, D'Orazio LM, Pachicano M, et al. Blood-brain barrier breakdown is an early biomarker of human cognitive dysfunction. Nat Med. 2019;25(2):270–6.
12. Benzinger TL, Blazey T, Jack CR Jr, Koeppe RA, Su Y, Xiong C, et al. Regional variability of imaging biomarkers in autosomal dominant Alzheimer's disease. Proc Natl Acad Sci U S A. 2013;110(47):E4502–E4509.
13. Lee S, Viqar F, Zimmerman ME, Narkhede A, Tosto G, Benzinger TL, et al. White matter hyperintensities are a core feature of Alzheimer's disease: Evidence from the dominantly inherited Alzheimer network. Ann Neurol. 2016;79(6):929–39.
14. Lee S, Zimmerman ME, Narkhede A, Nasrabady SE, Tosto G, Meier IB, et al. White matter hyperintensities and the mediating role of cerebral amyloid angiopathy in dominantly-inherited Alzheimer's disease. PLoS One. 2018;13(5):e0195838.
15. Love S, Miners JS. Cerebrovascular disease in ageing and Alzheimer's disease. Acta Neuropathol. 2016;131(5):645–58.
16. Nortley R, Korte N, Izquierdo P, Hirunpattarasilp C, Mishra A, Jaunmuktane Z, et al. Amyloid beta oligomers constrict human capillaries in Alzheimer's disease via signaling to pericytes. Science. 2019;365(6450):eaav9518.
17. Hald ES, Timm CD, Alford PW. Amyloid beta influences vascular smooth muscle contractility and mechanoadaptation. J Biomech Eng. 2016;138(11). https://doi.org/10.1115/1.4034560.
18. Marco S, Skaper SD. Amyloid beta-peptide1-42 alters tight junction protein distribution and expression in brain microvessel endothelial cells. Neurosci Lett. 2006;401(3):219–24.
19. Tai LM, Holloway KA, Male DK, Loughlin AJ, Romero IA. Amyloid-beta-induced occludin down-regulation and increased permeability in human brain endothelial cells is mediated by MAPK activation. J Cell Mol Med. 2010;14(5):1101–12.
20. Biron KE, Dickstein DL, Gopaul R, Jefferies WA. Amyloid triggers extensive cerebral angiogenesis causing blood brain barrier permeability and hypervascularity in Alzheimer's disease. PLoS One. 2011;6(8):e23789.
21. Hartz AM, Bauer B, Soldner EL, Wolf A, Boy S, Backhaus R, et al. Amyloid-beta contributes to blood-brain barrier leakage in transgenic human amyloid precursor protein mice and in humans with cerebral amyloid angiopathy. Stroke. 2012;43(2):514–23.
22. Barker R, Ashby EL, Wellington D, Barrow VM, Palmer JC, Kehoe PG, et al. Pathophysiology of white matter perfusion in Alzheimer's disease and vascular dementia. Brain. 2014;137(Pt 5):1524–32.
23. Thomas T, Miners S, Love S. Post-mortem assessment of hypoperfusion of cerebral cortex in Alzheimer's disease and vascular dementia. Brain. 2015;138(Pt 4):1059–69.
24. Miners JS, Palmer JC, Love S. Pathophysiology of hypoperfusion of the precuneus in early Alzheimer's disease. Brain Pathol. 2016;26(4):533–41.
25. Miners JS, Schulz I, Love S. Differing associations between Abeta accumulation, hypoperfusion, blood-brain barrier dysfunction and loss of PDGFRB pericyte marker in the precuneus and parietal white matter in Alzheimer's disease. J Cereb Blood Flow Metab. 2018;38(1):103–15.
26. Barker R, Wellington D, Esiri MM, Love S. Assessing white matter ischemic damage in dementia patients by measurement of myelin proteins. J Cereb Blood Flow Metab. 2013;33(7):1050–7.
27. Love S, Miners JS. Cerebral hypoperfusion and the energy deficit in Alzheimer's disease. Brain Pathol. 2016;26(5):607–17.
28. Palmer JC, Barker R, Kehoe PG, Love S. Endothelin-1 is elevated in Alzheimer's disease and upregulated by amyloid-beta. J Alzheimers Dis. 2012;29(4):853–61.
29. Montine TJ, Phelps CH, Beach TG, Bigio EH, Cairns NJ, Dickson DW, et al. National Institute on Aging-Alzheimer's Association guidelines for the neuropathologic assessment of Alzheimer's disease: a practical approach. Acta Neuropathol. 2012;123(1):1–11.
30. Chalmers K, Wilcock GK, Love S. APOE epsilon 4 influences the pathological phenotype of Alzheimer's disease by favouring cerebrovascular over parenchymal accumulation of A beta protein. Neuropathol Appl Neurobiol. 2003;29(3):231–8.
31. Olichney JM, Hansen LA, Hofstetter CR, Lee JH, Katzman R, Thal LJ. Association between severe cerebral amyloid angiopathy and cerebrovascular lesions in Alzheimer disease is not a

spurious one attributable to apolipoprotein E4. Arch Neurol. 2000;57(6):869–74.
32. Alafuzoff I, Pikkarainen M, Arzberger T, Thal DR, Al-Sarraj S, Bell J, et al. Inter-laboratory comparison of neuropathological assessments of β-amyloid protein: a study of the BrainNet Europe consortium. Acta Neuropathol. 2008;115(5):533–46.
33. Braak H, Alafuzoff I, Arzberger T, Kretzschmar H, Del Tredici K. Staging of Alzheimer disease-associated neurofibrillary pathology using paraffin sections and immunocytochemistry. Acta Neuropathol. 2006;112(4):389–404.
34. Miners JS, Jones R, Love S. Differential changes in Abeta42 and Abeta40 with age. J Alzheimers Dis. 2014;40(3):727–35.
35. Swirski M, Miners JS, de Silva R, Lashley T, Ling H, Holton J, et al. Evaluating the relationship between amyloid-beta and alpha-synuclein phosphorylated at Ser129 in dementia with Lewy bodies and Parkinson's disease. Alzheimers Res Ther. 2014;6(5–8):77.
36. van Helmond Z, Miners JS, Kehoe PG, Love S. Oligomeric Abeta in Alzheimer's disease: relationship to plaque and tangle pathology, APOE genotype and cerebral amyloid angiopathy. Brain Pathol. 2010;20(2):468–80.
37. van Helmond Z, Miners JS, Kehoe PG, Love S. Higher soluble amyloid beta concentration in frontal cortex of young adults than in normal elderly or Alzheimer's disease. Brain Pathol. 2010;20(4):787–93.
38. Reinstrup P, Ryding E, Ohlsson T, Dahm PL, Uski T. Cerebral blood volume (CBV) in humans during normo- and hypocapnia: influence of nitrous oxide (N(2)O). Anesthesiology. 2001;95(5):1079–82.
39. Korczyn AD, Vakhapova V, Grinberg LT. Vascular dementia. J Neurol Sci. 2012;322(1–2):2–10.
40. Thal DR, Grinberg LT, Attems J. Vascular dementia: different forms of vessel disorders contribute to the development of dementia in the elderly brain. Exp Gerontol. 2012;47(11):816–24.
41. Bourassa P, Tremblay C, Schneider JA, Bennett DA, Calon F. Brain mural cell loss in the parietal cortex in Alzheimer's disease correlates with cognitive decline and TDP-43 pathology. Neuropathol Appl Neurobiol. 2020;46(5):458–77.
42. Thammisetty SS, Pedragosa J, Weng YC, Calon F, Planas A, Kriz J. Age-related deregulation of TDP-43 after stroke enhances NF-kappaB-mediated inflammation and neuronal damage. J Neuroinflammation. 2018;15(1):312.
43. Miners S, Moulding H, de Silva R, Love S. Reduced vascular endothelial growth factor and capillary density in the occipital cortex in dementia with Lewy bodies. Brain Pathol. 2014;24(4):334–43.
44. Narushima I, Kita T, Kubo K, Yonetani Y, Momochi C, Yoshikawa I, et al. Highly enhanced permeability of blood-brain barrier induced by repeated administration of endothelin-1 in dogs and rats. Pharmacol Toxicol. 2003;92(1):21–6.
45. Narushima I, Kita T, Kubo K, Yonetani Y, Momochi C, Yoshikawa I, et al. Contribution of endothelin-1 to disruption of blood-brain barrier permeability in dogs. Naunyn Schmiedebergs Arch Pharmacol. 1999;360(6):639–45.
46. Zhang X, Yeung PK, McAlonan GM, Chung SS, Chung SK. Transgenic mice over-expressing endothelial endothelin-1 show cognitive deficit with blood-brain barrier breakdown after transient ischemia with long-term reperfusion. Neurobiol Learn Mem. 2013;101:46–54.
47. Reijerkerk A, Lakeman KA, Drexhage JA, van Het Hof B, van Wijck Y, van der Pol SM, et al. Brain endothelial barrier passage by monocytes is controlled by the endothelin system. J Neurochem. 2012;121(5):730–7.
48. Leung JW, Chung SS, Chung SK. Endothelial endothelin-1 over-expression using receptor tyrosine kinase tie-1 promoter leads to more severe vascular permeability and blood brain barrier breakdown after transient middle cerebral artery occlusion. Brain Res. 2009;1266:121–9.
49. Lo AC, Chen AY, Hung VK, Yaw LP, Fung MK, Ho MC, et al. Endothelin-1 overexpression leads to further water accumulation and brain edema after middle cerebral artery occlusion via aquaporin 4 expression in astrocytic end-feet. J Cereb Blood Flow Metab. 2005;25(8):998–1011.
50. Rosenberg GA. Neurological diseases in relation to the blood-brain barrier. J Cereb Blood Flow Metab. 2012;32(7):1139–51.
51. Ueno M, Chiba Y, Matsumoto K, Murakami R, Fujihara R, Kawauchi M, et al. Blood-brain barrier damage in vascular dementia. Neuropathology. 2016;36(2):115–24.
52. Wallin A, Blennow K, Fredman P, Gottfries CG, Karlsson I, Svennerholm L. Blood brain barrier function in vascular dementia. Acta Neurol Scand. 1990;81(4):318–22.

## SUPPORTING INFORMATION

Additional supporting information may be found online in the Supporting Information section.
Supplementary Material

**FIGURE S1** MAG:PLP1 and VEGF levels are inversely correlated in the frontal and parietal cortex and underlying white matter. (A-D) Scatterplots showing the relationship between MAG:PLP1 and VEGF in the frontal cortex (FC), parietal cortex (PC), frontal white matter (FWM) and parietal white matter (PWM). The solid line indicates best-fit linear regression and the interrupted lines the 95% confidence intervals. Each point represents a separate brain. Pearson's correlation coefficients are shown only for statistically significant relationships. $*p < 0.05$, $**p < 0.01$

**FIGURE S2** Relationships between markers of cerebral perfusion (MAG:PLP1 and VEGF) and Aβ (insoluble Aβ42 and Aβ40 levels, and parenchymal Aβ load) in frontal and parietal cortex. (A-L) Scatterplots showing the relationships of MAG:PLP1 and VEGF to Aβ42, Aβ40 and parenchymal Aβ load in the frontal cortex (FC) and parietal cortex (PC). The solid line indicates best-fit linear regression and the interrupted lines the 95% confidence intervals. Each point represents a separate brain. Pearson's correlation coefficients are shown only for statistically significant relationships. $*p < 0.05$, $***p < 0.001$

**FIGURE S3** Markers of cerebral hypoperfusion (MAG:PLP1 and VEGF) in relation to Braak tangle stage, phospho-tau load, endothelin-1, CAA and SVD severity in frontal and parietal cortex. (A-D) Scatterplots showing MAG:PLP1 and VEGF-A in relation to Braak tangle stage (BS). (E-H) Scatterplots showing the relationship of MAG:PLP1 and VEGF-A to phospho-tau (AT8) load. (I-L) Scatterplots showing the relationship of MAG:PLP1 and VEGF-A to endothelin-1 (EDN1) level. (M-P) Scatterplots showing MAG:PLP1 and VEGF-A in relation to cerebral amyloid angiopathy (CAA) severity. (Q-T) Scatterplots showing the relationship of MAG:PLP1 and VEGF-A to severity of small vessel disease (SVD). In the scatterplots subdivided according to Braak tangle stage, CAA or SVD severity, the horizontal bars represent the mean ± standard error of the mean

(SEM). One-way ANOVA with Bonferroni post-hoc analysis was used to determine if MAG:PLP1 or VEGF was altered in relation to Braak tangle stage (0-II, III-IV, V-VI), cerebral amyloid angiopathy (CAA) score (0, 1, 2, 3) or small vessel disease (SVD) (0, 1, 2, 3). In the scatterplots, the solid line indicates best-fit linear regression and the interrupted lines the 95% confidence intervals. Pearson's correlation coefficients are shown only for statistically significant relationships. Each point represents a separate brain. *$p < 0.05$, **$p < 0.001$, ****$p < 0.0001$

**FIGURE S4** Relationship between markers of cerebral hypoperfusion (MAG:PLP1 and VEGF) and Aβ (insoluble Aβ42 and Aβ40, and parenchymal Aβ load) in frontal and parietal white matter. (A-O) Scatterplots showing the relationship of MAG:PLP1 and VEGF to insoluble cortical Aβ42 and Aβ40 and parenchymal Aβ load, and to insoluble Aβ42 within the white matter. FC – frontal cortex, PC – parietal cortex, FWM – frontal white matter, PWM – parietal white matter. The solid line indicates best-fit linear regression and the interrupted lines the 95% confidence intervals. Pearson's correlation coefficients are shown only for statistically significant relationships. Each point represents a separate brain. *$p < 0.05$, **$p < 0.01$

**FIGURE S5** Markers of cerebral hypoperfusion (MAG:PLP1, VEGF) in relation to Braak tangle stage, phospho-tau load, endothelin-1, CAA and SVD severity in frontal and parietal white matter. (A-D) Scatterplots showing MAG:PLP1 and VEGF-A in relation to Braak tangle stage (BS). (E-H) Scatterplots showing the relationship of MAG:PLP1 and VEGF-A to phospho-tau (AT8) load. (I-P) Scatterplots showing the relationship of MAG:PLP and VEGF-A to cortical and white matter endothelin-1 (EDN1) levels. (Q-T) Scatterplots showing MAG:PLP1 and VEGF-A in relation to cerebral amyloid angiopathy (CAA) severity. (V-Y) Scatterplots showing MAG:PLP1 and VEGF-A in relation to small vessel disease (SVD). FC – frontal cortex, PC – parietal cortex, FWM – frontal white matter, PWM – parietal white matter. In the scatterplots subdivided according to Braak tangle stage, CAA or SVD severity, the horizontal bars represent the mean ± standard error of the mean (SEM). One-way ANOVA with Bonferroni post-hoc analysis was used to determine if MAG:PLP1 or VEGF was altered in relation to Braak tangle stage (0-II, III-IV, V-VI), cerebral amyloid angiopathy (CAA) score (0, 1, 2, 3) or small vessel disease (SVD) (0, 1, 2, 3). In the scatterplots the solid line indicates best-fit linear regression and the interrupted lines the 95% confidence intervals. Pearson's correlation coefficients are shown only for statistically significant relationships. Each point represents a separate brain. *$p < 0.05$, **$p < 0.001$, ****$p < 0.0001$

**TABLE S1** Insoluble Aβ42 and Aβ40, and parenchymal Aβ and phospho-tau loads, in frontal and parietal cortex. Aβ42 and Aβ40 levels were measured by ELISA in guandine-extracts representing the insoluble Aβ fraction. Parenchymal Aβ was immunolabelled with 4G8 and phospho-tau was immunolabelled with AT8. Mean Aβ and phospho-tau loads were quantified by field-fraction analysis using computer-based image analysis software (Image-Pro Plus 7, Media Cybernetics). The values are shown as mean ± SEM. *significant difference between control and AD, #significant difference between AD and mixed dementia. #$p < 0.05$, ##$p < 0.01$, ***$p < 0.001$, ****$p < 0.0001$

**TABLE S2** List of MRC UK-BBN identifier numbers for cases used in this study. AD, Alzheimer's disease; VaD, Vascular dementia

**How to cite this article:** Tayler H, Miners JS, Güzel Ö, MacLachlan R, Love S. Mediators of cerebral hypoperfusion and blood-brain barrier leakiness in Alzheimer's disease, vascular dementia and mixed dementia. *Brain Pathology*. 2021;31:e12935. https://doi.org/10.1111/bpa.12935